Continuous-Thrust Analytical State Propagation for J2-Perturbed Two-Body Problem

Abstract: The continuous-thrust analytical state propagation for J_2-perturbed two-body problem is proposed under general thrust acceleration. For both the periodic and non-periodic cases, the real thrust acceleration is approximated by a truncated Fourier series in terms of eccentric anomaly. An approximation of the real orbital motion is obtained by the secular motion and the periodic motion oscillating around the secular one. The analytical propagation of the secular orbital motion is derived based on the orbital average method and the thrust series approximation. Based on the obtained analytical secular propagation, the periodic motion equations are obtained by performing the first-order Taylor expansion of the real motion around the secular motion, and then the analytical solution to the periodic motion is presented by using the linear system theory. Several numerical examples are provided to verify that the analytical propagation accuracy can be effectively improved by considering the periodic orbital variation on the basis of the secular orbital motion.

1. Introduction

For spacecraft orbital dynamics and control under continuous thrust, the problems can be mainly divided into two categories: a) the orbital initial value problem (also called forward problem) that propagates the orbital state under a given thrust; b) the orbital boundary value problem (also called inverse problem) that solves the desired thrust with given initial and terminal states. Continuous-thrust analytical orbital state propagation can be used not only for efficiently solving the initial value problem [1], but also for the boundary value problem, e.g., trajectory optimization problem [2], hence it has received extensive attention from scholars.

Continuous-thrust analytical state propagation has been proposed for many cases with different orbital motion models and thrust acceleration forms. A classical case is

that the constant thrust acceleration is applied along some fixed direction in the absolute orbital motion model. Three common thrust directions are radial, tangential, and circumferential directions. For radial thrust, explicit solutions are obtained in terms of elliptic integrals [3][4] and Weierstrass functions [5]. Based on the explicit solutions, Kaki and Akella [6] designed an analytical guidance method for the rephasing problem. In addition, Multiple scales asymptotic method [7] and homotopy perturbation method [8] are used to obtain the analytical approximate solutions. For tangential thrust, Benney [9] investigated the escape problem from a circular orbit and proposed an approximate solution. Gao and Kluever [10] obtained an analytical average solution by using the orbital average method. By approximating the real trajectory with a mean trajectory and a trajectory oscillating around the mean one, Perkins [11] presented an approximate solution of the trajectory starting from a circular orbit. For circumferential thrust, Tsien [3] also studied the problem and proposed an approximate solution. Battin [4] and Niccolai et al. [12] presented the approximate solutions for the circular and elliptical parking orbits, respectively. In addition, there are also some analytical solutions for other thrust directions, e.g., velocity-normal direction [13], orbit-normal direction [14], and any fixed direction in the orbital plane [15].

Continuous-thrust analytical state propagation can be also obtained for some other cases, e.g., the thrust acceleration is not constant but varies according to some special law. Considering the ratio of the thrust acceleration to the gravitational acceleration, when this ration is fixed, Boltz [16][17] presented analytical approximate solutions for the radial and tangential thrust; whereas when this ration varies with the flight direction angle, Roa et al. [18] proposed an alternative analytical solution for the tangential thrust. The above studies are for the absolute orbital motion. For linear relative motion, there are usually two orbital dynamical models according to the type of reference orbit: the time-invariant model for circular reference orbits and the time-varying model for elliptical reference orbits. For constant thrust acceleration, analytical state propagation expressions are presented for circular reference orbits [19] and elliptical reference orbits [20]. However, in the preceding studies, there are some restrictions on the thrust

acceleration, e.g., keeping constant or varying according to a particular law.

For general continuous thrust, there are some existing results of analytical state propagation for different orbital motion models. For relative motion model, Gazzino and Gurfil [21] proposed the analytical propagation of relative mean orbital elements under out-of-plane thrust acceleration. Based on the thrust series approximation, Lin and Zhang [22] presented the analytical state propagation for the linear relative motion in elliptical orbits, and the research is further extended to the second-order relative motion accounting for J_2 perturbation [23]. For absolute motion model, Hudson and Scheeres [24] expressed the thrust acceleration as a truncated Fourier series in terms of eccentric anomaly, and applied the orbital average method to obtain the analytical secular propagation, which gives mean orbital elements as the function of fourteen thrust Fourier coefficients (TFCs). Based on the obtained secular propagation, Ko and Scheeres [25] analyzed the impact of fourteen TFCs on the variation rates of orbital elements, and proposed an essential coefficient set containing only six TFCs. In addition, Nie and Gurfil [26] expressed the thrust acceleration as a Fourier series in terms of mean anomaly instead of eccentric anomaly, and presented alternative secular propagation expressions of mean orbital elements by using the orbital average method. However, in the preceding studies [24][25][26] of continuous-thrust analytical state propagation for absolute orbital motion, only the secular orbital motion is considered by using the orbital average method, which will lead to the decrease of propagation accuracy when the orbital variation within one orbital period is relatively large. Moreover, the effects of perturbations, e.g., J_2 perturbation, are not considered.

In this paper, the analytical state propagation for absolute orbital motion is proposed under general continuous thrust accounting for J_2 perturbation. The real thrust acceleration is approximated by a truncated Fourier series in terms of eccentric anomaly. The real orbital motion is split into two parts: the secular (mean) orbital motion and the periodic orbital motion oscillating around the secular one. Based on the thrust series approximation, the analytical solution to secular orbital motion is obtained by using the orbital average method. The periodic orbital motion is derived by taking the first-order

Taylor expansion of the real orbit around the secular orbit, and then the analytical solution is obtained based on the linear system theory. The main contribution of this paper is twofold:

1) continuous-thrust analytical state propagation under general thrust is proposed for absolute orbital motion, where both the secular and periodic orbital variations, rather than solely the secular variation, are taken into account to improve the propagation accuracy;
2) the effect of J_2 perturbation is further included to derive the continuous-thrust analytical state propagation for absolute orbital motion.

2. Orbital propagation model

For the J_2-perturbed two-body problem, the orbital motion under general continuous thrust can be described by using the Gauss variation equations (GVEs) [27],

$$\begin{cases} \dfrac{\mathrm{d}a}{\mathrm{d}t} = \dfrac{2\sqrt{a^3}}{\eta\sqrt{\mu}}(e\sin\varphi F_r + \rho F_s) \\ \dfrac{\mathrm{d}e}{\mathrm{d}t} = \dfrac{\eta\sqrt{a}}{\sqrt{\mu}}\left[\sin\varphi F_r + \left(\dfrac{e+\cos\varphi}{\rho}+\cos\varphi\right)F_s\right] \\ \dfrac{\mathrm{d}i}{\mathrm{d}t} = \dfrac{\eta\sqrt{a}}{\sqrt{\mu}}\dfrac{\cos(\varphi+\omega)}{\rho}F_w \\ \dfrac{\mathrm{d}\Omega}{\mathrm{d}t} = \dfrac{\eta\sqrt{a}}{\sqrt{\mu}}\dfrac{\sin(\varphi+\omega)}{\rho\sin i}F_w \\ \dfrac{\mathrm{d}\omega}{\mathrm{d}t} = \dfrac{\eta\sqrt{a}}{\sqrt{\mu}}\left(-\dfrac{\cos\varphi}{e}F_r + \dfrac{1+\rho}{e\rho}\sin\varphi F_s - \dfrac{\cos i\sin(\varphi+\omega)}{\rho\sin i}F_w\right) \\ \dfrac{\mathrm{d}M}{\mathrm{d}t} = n + \dfrac{\eta^2\sqrt{a}}{e\sqrt{\mu}}\left(\dfrac{\rho\cos\varphi-2e}{\rho}F_r - \dfrac{1+\rho}{\rho}\sin\varphi F_s\right) \end{cases} \tag{1}$$

where a is semi-major axis, e is eccentricity, i is inclination, ω is argument of perigee, Ω is right ascension of the ascending node, φ is true anomaly, M is mean anomaly. $\eta=\sqrt{1-e^2}$, $\rho=1+e\cos\varphi$, $n=\sqrt{\mu/a^3}$ is mean motion rate, μ is the standard gravitational parameter, and $\boldsymbol{F}=F_r\hat{\boldsymbol{r}}+F_s\hat{\boldsymbol{s}}+F_w\hat{\boldsymbol{w}}$ is disturbed acceleration and expressed in the RSW coordinate frame, where the $\hat{\boldsymbol{r}}$, $\hat{\boldsymbol{s}}$, and $\hat{\boldsymbol{w}}$

axes point along the orbital radial, circumferential, and normal directions, respectively.

In this paper, the disturbed acceleration is composed of two parts: the thrust acceleration and the J_2-perturbed acceleration, i.e.,

$$\begin{cases} F_r = u_r + F_{J2,r} \\ F_s = u_s + F_{J2,s} \\ F_w = u_w + F_{J2,w} \end{cases} \tag{2}$$

where (u_r, u_s, u_w) and $(F_{J2,r}, F_{J2,s}, F_{J2,w})$ denote the components of the thrust acceleration and the J_2-perturbed acceleration in the RSW coordinate frame, respectively. The expression of the J_2-perturbed acceleration is [27]

$$\begin{cases} F_{J2,r} = -\dfrac{3\mu J_2 R_\oplus^2}{2r^4}[1-3\sin^2 i \sin^2(\omega+\varphi)] \\ F_{J2,s} = -\dfrac{3\mu J_2 R_\oplus^2}{r^4}\sin^2 i \sin(\omega+\varphi)\cos(\omega+\varphi) \\ F_{J2,w} = -\dfrac{3\mu J_2 R_\oplus^2}{r^4}\sin i \cos i \sin(\omega+\varphi) \end{cases} \tag{3}$$

where $R_\oplus = 6378.14$ km denotes the Earth's mean radius, $J_2 = 1.082627 \times 10^{-3}$, and r denotes the orbital radius.

Assume that the real orbital motion is approximated by the secular motion and the periodic motion oscillating around the secular one, i.e.,

$$x(t) \approx x_s(t) + x_p(t) \tag{4}$$

where x denotes any orbital element, $x_s(t) = x(t_0) + \bar{\dot{x}} \cdot (t - t_0)$ and $x_p(t)$ denote the secular and periodic orbital motions, respectively, and where t_0 is the initial time point and $\bar{\dot{x}}$ is the secular variation rate of the orbital element under thrust acceleration and J_2 perturbation. In the following two sections, the analytical propagation of the secular orbital motion is first derived based on the orbital average theory and the thrust series approximation, and then the analytical propagation of the periodic orbital motion is further obtained by using the first-order Taylor expansion and the linear system theory.

3. Analytical propagation of secular orbital motion

For simplicity, the coupling between the J_2 perturbation and the thrust acceleration

is ignored, and then the secular variation rate of the orbital element is approximated as

$$\bar{\dot{x}} \approx \bar{\dot{x}}_u + \bar{\dot{x}}_{J2} \tag{5}$$

where $\bar{\dot{x}}_u$ and $\bar{\dot{x}}_{J2}$ denote the secular variation rates of the orbital element under the thrust acceleration solely and the J_2 perturbation solely, respectively. The secular variation rates of orbital elements solely under J_2 perturbation are [27]

$$\begin{pmatrix} \bar{\dot{a}}_{J2} \\ \bar{\dot{e}}_{J2} \\ \bar{\dot{i}}_{J2} \\ \bar{\dot{\Omega}}_{J2} \\ \bar{\dot{\omega}}_{J2} \\ \bar{\dot{M}}_{J2} \end{pmatrix} = \gamma \begin{pmatrix} 0 \\ 0 \\ 0 \\ -2\cos i \\ 5\cos^2 i - 1 \\ \eta(3\cos^2 i - 1) \end{pmatrix} \tag{6}$$

where $\gamma = J_R \Big/ \left(a^{7/2}\eta^4\right)$, and where $J_R = 3J_2 R_\oplus^2 \sqrt{\mu}/4$.

Based on the orbital average theory, the secular variation rate of the orbital element solely under thrust acceleration within a time period $[t_0, t_1]$ is

$$\bar{\dot{x}}_u = \frac{1}{\Delta T}\int_{t_0}^{t_1} \dot{x}_u \, \mathrm{d}t \tag{7}$$

where $\Delta T = t_1 - t_0$, and $\dot{x}_u$ denotes the instantaneous orbital variation rate only under thrust acceleration, which is obtained from the GVEs in Eq. (1). Based on the following relationship [23],

$$\mathrm{d}t = \frac{1 - e\cos E}{n}\mathrm{d}E \tag{8}$$

where E is eccentric anomaly, Eq. (7) can be rewritten as

$$\bar{\dot{x}}_u = \frac{1}{n\Delta T}\int_{E_0}^{E_1} (1 - e\cos E)\dot{x}_u \, \mathrm{dE} \tag{9}$$

Substituting Eq. (1) into Eq. (9) yields

$$\bar{\dot{a}}_u = \frac{2\sqrt{a^3}}{n\Delta T\sqrt{\mu}}\int_{E_0}^{E_1} (e\sin E u_r + \eta u_s)\, \mathrm{d}E \tag{10}$$

$$\bar{\dot{e}}_u = \frac{\eta\sqrt{a}}{n\Delta T\sqrt{\mu}}\int_{E_0}^{E_1} \left[\eta\sin E u_r + \left(2\cos E - \frac{3}{2}e - \frac{1}{2}e\cos(2E)\right)u_s\right]\mathrm{d}E \tag{11}$$

$$\bar{\dot{i}}_u = \frac{\sqrt{a}}{2n\Delta T\eta\sqrt{\mu}}\int_{E_0}^{E_1} u_w\Big[2(1+e^2)\cos\omega\cos E - 3e\cos\omega - 2\eta\sin\omega\sin E - e\cos\omega\cos(2E) + e\eta\sin\omega\sin(2E)\Big]\mathrm{d}E \tag{12}$$

$$\bar{\dot{\Omega}}_u = \frac{\sqrt{a}}{2n\Delta T\eta\sqrt{\mu}\sin i}\int_{E_0}^{E_1} u_w\Big[2\eta\cos\omega\sin E + 2(1+e^2)\sin\omega\cos E - 3e\sin\omega - e\eta\cos\omega\sin(2E) - e\sin\omega\cos(2E)\Big]\mathrm{d}E \tag{13}$$

$$\begin{aligned}\bar{\dot{\omega}}_u &= -\bar{\dot{\Omega}}_u\cos i + \frac{\sqrt{a}}{en\Delta T\sqrt{\mu}}\int_{E_0}^{E_1} -\eta(\cos E - e)u_r\,\mathrm{d}E \\ &\quad + \frac{\sqrt{a}}{en\Delta T\sqrt{\mu}}\int_{E_0}^{E_1}\left[(2-e^2)\sin E - \frac{1}{2}e\sin(2E)\right]u_s\,\mathrm{d}E\end{aligned} \tag{14}$$

$$\begin{aligned}\bar{\dot{M}}_u &= n + \frac{\sqrt{a}}{n\Delta Te\sqrt{\mu}}\int_{E_0}^{E_1}\Big[(1+3e^2)\cos E - e^3\cos(2E) - 3e\Big]u_r\,\mathrm{d}E \\ &\quad - \frac{\eta\sqrt{a}}{2n\Delta Te\sqrt{\mu}}\int_{E_0}^{E_1}\Big[2(2-e^2)\sin E - e\sin(2E)\Big]u_s\,\mathrm{d}E\end{aligned} \tag{15}$$

The analytical expressions of the integrals in Eq. (10)~Eq. (15) are derived based on the thrust series approximation in this section.

When the real thrust acceleration within the interval $[E_0, E_1]$ is periodic with respect to eccentric anomaly E, it is approximated by using the truncated Fourier series with respect to E,

$$\begin{cases} u_r = \sum_{j=0}^{N_r}\kappa_{r,j}\cos(jLE) + \sum_{j=1}^{N_r}\kappa_{r,j+N_r}\sin(jLE) \\ u_s = \sum_{j=0}^{N_s}\kappa_{s,j}\cos(jLE) + \sum_{j=1}^{N_s}\kappa_{s,j+N_s}\sin(jLE) \\ u_w = \sum_{j=0}^{N_w}\kappa_{w,j}\cos(jLE) + \sum_{j=1}^{N_w}\kappa_{w,j+N_w}\sin(jLE) \end{cases} \tag{16}$$

where $L = 2\pi/(E_1 - E_0)$, N_χ $(\chi = r, s, w)$ denotes the thrust series truncation order, and $\kappa_{\chi,j}$ $(j = 0,1,\ldots,2N_\chi)$ denotes the thrust series coefficient, which is obtained by using the discrete least-square approximation method [28]. In addition, when the real thrust acceleration within the interval $[E_0, E_1]$ is not periodic, it is extended to the interval $[E_0, E_2]$, where $E_2 = 2E_1 - E_0$, and the thrust acceleration within the interval $[E_1, E_2]$ is an even symmetry of that within the interval $[E_0, E_1]$. And then, the truncated Fourier series approximation of the real thrust acceleration within the interval

$[E_0, E_1]$ is also obtained with $L = \pi / (E_1 - E_0)$. The obtained thrust Fourier series approximation is then substituted into Eq. (10)~Eq. (15) to give

$$\bar{\dot{a}}_u = \frac{2\sqrt{a^3}}{n\sqrt{\mu}\Delta T}\left(\sum_{j=0}^{2N_r} em_{3,j}\kappa_{r,j} + \sum_{j=0}^{2N_s}\eta m_{1,j}\kappa_{s,j}\right) \tag{17}$$

$$\bar{\dot{e}}_u = \frac{\eta\sqrt{a}}{n\sqrt{\mu}\Delta T}\left[\sum_{j=0}^{2N_r}\eta m_{3,j}\kappa_{r,j} + \sum_{j=0}^{2N_s}\left(2m_{2,j} - \frac{3}{2}em_{1,j} - \frac{1}{2}em_{4,j}\right)\kappa_{s,j}\right] \tag{18}$$

$$\begin{aligned}\bar{\dot{i}}_u = {} & \frac{\sqrt{a}}{2n\eta\sqrt{\mu}\Delta T}\sum_{j=0}^{2N_w}\left[2(1+e^2)\cos\omega m_{2,j} - 3e\cos\omega m_{1,j}\right]\kappa_{w,j} \\ & + \frac{\sqrt{a}}{2n\eta\sqrt{\mu}\Delta T}\sum_{j=0}^{2N_w}\left(-2\eta\sin\omega m_{3,j} - e\cos\omega m_{4,j} + e\eta\sin\omega m_{5,j}\right)\kappa_{w,j}\end{aligned} \tag{19}$$

$$\begin{aligned}\bar{\dot{\Omega}}_u = {} & \frac{\sqrt{a}}{2n\eta\Delta T\sqrt{\mu}\sin i}\sum_{j=0}^{2N_w}\left[2\eta\cos\omega m_{3,j} + 2(1+e^2)\sin\omega m_{2,j}\right]\kappa_{w,j} \\ & + \frac{\sqrt{a}}{2n\eta\Delta T\sqrt{\mu}\sin i}\sum_{j=0}^{2N_w}\left(-3e\sin\omega m_{1,j} - e\eta\cos\omega m_{5,j} - e\sin\omega m_{4,j}\right)\kappa_{w,j}\end{aligned} \tag{20}$$

$$\bar{\dot{\omega}}_u = -\bar{\dot{\Omega}}_u\cos i + \frac{\sqrt{a}}{en\Delta T\sqrt{\mu}}\sum_{j=0}^{2N_r}\left[-\eta m_{2,j} + \eta em_{1,j} + (2-e^2)m_{3,j} - \frac{e}{2}m_{5,j}\right]\kappa_{r,j} \tag{21}$$

$$\begin{aligned}\bar{\dot{M}}_u = {} & n + \frac{\sqrt{a}}{ne\Delta T\sqrt{\mu}}\sum_{j=0}^{2N_r}\left[(1+3e^2)m_{2,j} - e^3m_{4,j} - 3em_{1,j}\right]\kappa_{r,j} \\ & - \frac{\eta\sqrt{a}}{2ne\Delta T\sqrt{\mu}}\sum_{j=0}^{2N_s}\left[2(2-e^2)m_{3,j} - em_{5,j}\right]\kappa_{s,j}\end{aligned} \tag{22}$$

where

$$\begin{cases} m_{1,j} = \int_{E_0}^{E_1} f(jLE)\,\mathrm{d}E \\ m_{2,j} = \int_{E_0}^{E_1} f(jLE)\cos E\,\mathrm{d}E \\ m_{3,j} = \int_{E_0}^{E_1} f(jLE)\sin E\,\mathrm{d}E \\ m_{4,j} = \int_{E_0}^{E_1} f(jLE)\cos(2E)\,\mathrm{d}E \\ m_{5,j} = \int_{E_0}^{E_1} f(jLE)\sin(2E)\,\mathrm{d}E \end{cases} \tag{23}$$

and where

$$f(jLE)=\begin{cases}\cos(jLE), & \text{if } 0\le j\le N_\chi\\ \sin[(j-N_\chi)LE], & \text{if } N_\chi+1\le j\le 2N_\chi\end{cases} \tag{24}$$

The integrals in Eq. (23) can be obtained from the following relationships:

$$\int_{E_0}^{E_1}\cos(b_1E)\cos(b_2E)\,\mathrm{d}E=\begin{cases}\left.\dfrac{E}{2}+\dfrac{\sin[(b_1+b_2)E]}{2(b_1+b_2)}\right|_{E_0}^{E_1}, & \text{if } b_1=b_2\\ \left.\dfrac{\sin[(b_1-b_2)E]}{2(b_1-b_2)}+\dfrac{\sin[(b_1+b_2)E]}{2(b_1+b_2)}\right|_{E_0}^{E_1}, & \text{if } b_1\ne b_2\end{cases} \tag{25}$$

$$\int_{E_0}^{E_1}\cos(b_1E)\sin(b_2E)\,\mathrm{d}E=\begin{cases}\left.-\dfrac{\cos[(b_2+b_1)E]}{2(b_2+b_1)}\right|_{E_0}^{E_1}, & \text{if } b_1=b_2\\ \left.-\dfrac{\cos[(b_2+b_1)E]}{2(b_2+b_1)}-\dfrac{\cos[(b_2-b_1)E]}{2(b_2-b_1)}\right|_{E_0}^{E_1}, & \text{if } b_1\ne b_2\end{cases} \tag{26}$$

$$\int_{E_0}^{E_1}\sin(b_1E)\sin(b_2E)\,\mathrm{d}E=\begin{cases}\left.\dfrac{E}{2}-\dfrac{\sin[(b_1+b_2)E]}{2(b_1+b_2)}\right|_{E_0}^{E_1}, & \text{if } b_1=b_2\\ \left.\dfrac{\sin[(b_1-b_2)E]}{2(b_1-b_2)}-\dfrac{\sin[(b_1+b_2)E]}{2(b_1+b_2)}\right|_{E_0}^{E_1}, & \text{if } b_1\ne b_2\end{cases} \tag{27}$$

Based on Eq. (5), Eq. (6) and Eq. (17)-Eq. (22), one can obtain the analytical approximation expressions of the secular variation rates of orbital elements under thrust acceleration and J_2 perturbation. The analytical propagation of the secular orbital motion can be obtained as

$$\begin{cases}a_s(t)=a(t_0)+\bar{\dot{a}}\cdot(t-t_0)\\ e_s(t)=e(t_0)+\bar{\dot{e}}\cdot(t-t_0)\\ i_s(t)=i(t_0)+\bar{\dot{i}}\cdot(t-t_0)\\ \Omega_s(t)=\Omega(t_0)+\bar{\dot{\Omega}}\cdot(t-t_0)\\ \omega_s(t)=\omega(t_0)+\bar{\dot{\omega}}\cdot(t-t_0)\\ M_s(t)=M(t_0)+\bar{\dot{M}}\cdot(t-t_0)\end{cases} \tag{28}$$

4. Analytical propagation for periodic orbital motion

Based on the secular orbital propagation in Sec. 3, the analytical propagation of the periodic orbital motion is obtained in this section. For this purpose, similarly, ignoring the coupling between the J_2 perturbation and the thrust acceleration, the

periodic orbital motion can be approximated as

$$x_p(t) \approx x_{p,u}(t) + x_{p,J2}(t) \tag{29}$$

where $x_{p,u}(t)$ and $x_{p,J2}(t)$ denote the periodic terms of orbital motion under thrust acceleration solely and J_2 perturbation solely, respectively. The periodic orbital motion under J_2 perturbation consists of several parts, e.g., the short-periodic term and the long-periodic term [27], and only the short-periodic term is considered in this paper to obtain an approximation of $x_{p,J2}(t)$. The expression of the short-periodic term of orbital motion under J_2 perturbation is [27]

$$a_{sp,J2}(\boldsymbol{x}_s) = \frac{J_2 R_\oplus^2}{a}\left\{\left(\frac{a}{r}\right)^3 - \frac{1}{\eta^3} + \left[-\left(\frac{a}{r}\right)^3 + \frac{1}{\eta^3} + \left(\frac{a}{r}\right)^3 c_{2\omega+2\varphi}\right]\frac{3s_i^2}{2}\right\} \tag{30}$$

$$e_{sp,J2}(\boldsymbol{x}_s) = \frac{J_2 R_\oplus^2}{4e}\left[\frac{-2}{a^2\eta} + \frac{2p}{r^3} + 3s_i^2\left(\frac{\eta - c_{2\omega+2\varphi}}{a^2\eta^2} - \frac{e\eta^2\sigma}{3p^2} - \frac{2ps_{\omega+\varphi}^2}{r^3}\right)\right] \tag{31}$$

$$i_{sp,J2}(\boldsymbol{x}_s) = \frac{J_2 R_\oplus^2 s_{2i}}{8p^2}\left(3c_{2\omega+2\varphi} + 3ec_{2\omega+\varphi} + ec_{2\omega+3\varphi}\right) \tag{32}$$

$$\Omega_{sp,J2}(\boldsymbol{x}_s) = -\frac{J_2 R_\oplus^2 c_i}{4p^2}\left[6(\varphi - M + es_\varphi) - 3s_{2\omega+2\varphi} - 3es_{2\omega+\varphi} - es_{2\omega+3\varphi}\right] \tag{33}$$

$$\begin{aligned}\omega_{sp,J2}(\boldsymbol{x}_s) = \frac{3J_2 R_\oplus^2}{4p^2}\Bigg\{&\left(1-\frac{3}{2}s_\varphi^2\right)\left[\left(\frac{2}{e}-\frac{e}{2}\right)s_\varphi + s_{2\varphi} + \frac{e}{6}s_{3\varphi}\right] + \frac{e}{8}s_i^2 s_{\varphi-2\omega} \\ &+\left(4-5s_i^2\right)(\varphi - M + es_\varphi) - \frac{2}{e}\left[\frac{1}{4}s_i^2 + \left(\frac{1}{2}-\frac{15}{16}s_i^2\right)e^2\right]s_{\varphi+2\omega} + \frac{e}{8}s_i^2 s_{5\varphi+2\omega} \\ &-\left(1-\frac{5}{2}s_i^2\right)s_{2\varphi+2\omega} + \frac{2}{e}\left[\frac{7}{12}s_i^2 - \frac{1}{6}\left(1-\frac{19}{8}s_i^2\right)e^2\right]s_{3\varphi+2\omega} + \frac{3}{4}s_i^2 s_{4\varphi+2\omega}\Bigg\}\end{aligned} \tag{34}$$

$$\begin{aligned}M_{sp,J2}(\boldsymbol{x}_s) = \frac{3J_2 R_\oplus^2 \eta}{2ep^2}\Bigg\{&-\left(1-\frac{3}{2}s_i^2\right)\left[\left(1-\frac{e^2}{4}\right)s_\varphi + \frac{e}{2}s_{2\varphi} + \frac{e^2}{12}s_{3\varphi}\right] \\ &+s_i^2\left[\left(\frac{1}{4}+\frac{5}{16}e^2\right)s_{\varphi+2\omega} - \frac{e^2}{16}s_{\varphi-2\omega} - \frac{7}{12}\left(1-\frac{e^2}{28}\right)s_{3\varphi+2\omega} - \frac{3e}{8}s_{4\varphi+2\omega} - \frac{e^2}{16}s_{5\varphi+2\omega}\right]\Bigg\}\end{aligned} \tag{35}$$

where $\boldsymbol{x}_s = [a_s, e_s, i_s, \Omega_s, \omega_s, M_s]^T$ denotes the secular orbital element vector obtained form Eq. (28), $c_\bullet = \cos(\bullet)$, $s_\bullet = \sin(\bullet)$, and $\sigma = 3c_{2\omega+\varphi} + c_{3\varphi+2\omega}$.

The periodic orbital motion solely under thrust acceleration can be expressed as

$$x_{p,u}(t) = x_u(t) - x_{s,u}(t) \tag{36}$$

where $x_{s,u}(t) = x(t_0) + \bar{\dot{x}}_u \cdot (t - t_0)$, and $x_u(t)$ denotes the orbital motion solely under thrust acceleration. Differentiating Eq. (36) with respect to time t gives

$$\dot{x}_{p,u}(t) = \dot{x}_u(t) - \bar{\dot{x}}_u \tag{37}$$

Based on Eq. (1), the above equation can be rewritten in the state-space form,

$$\dot{\boldsymbol{x}}_{p,u}(t) = \boldsymbol{g}(\boldsymbol{x}_u) + \boldsymbol{B}(\boldsymbol{x}_u)\boldsymbol{u}(t) - \bar{\dot{\boldsymbol{x}}}_u \tag{38}$$

where $\boldsymbol{x} = [a, e, i, \Omega, \omega, M]^T$ denotes the orbital element vector, $\bar{\dot{\boldsymbol{x}}}_u$ is obtained from Eq. (17)-Eq. (22), and

$$\boldsymbol{g}(\boldsymbol{x}_u) = [0, 0, 0, 0, 0, n]^T \tag{39}$$

$$\boldsymbol{B}(\boldsymbol{x}_u) = \frac{\eta\sqrt{a}}{\sqrt{\mu}} \begin{bmatrix} \frac{2ae s_\varphi}{\eta^2} & \frac{2a\rho}{\eta^2} & 0 \\ s_\varphi & \frac{e + c_\varphi}{\rho} + c_\varphi & 0 \\ 0 & 0 & \frac{c_{\varphi+\omega}}{\rho} \\ 0 & 0 & \frac{s_{\varphi+\omega}}{\rho \sin i} \\ -\frac{c_\varphi}{e} & \frac{1+\rho}{e\rho} s_\varphi & -\frac{c_i s_{\varphi+\omega}}{\rho s_i} \\ \frac{\eta}{e}\frac{\rho c_\varphi - 2e}{\rho} & -\frac{\eta}{e}\frac{1+\rho}{\rho} s_\varphi & 0 \end{bmatrix} \tag{40}$$

Performing the first-order Taylor expansion of $\boldsymbol{x}_u$ around $\boldsymbol{x}_{s,u}$, one gets

$$\dot{\boldsymbol{x}}_{p.u}(t) \approx \boldsymbol{A}(\boldsymbol{x}_{s,u})\boldsymbol{x}_{p.u}(t) + \boldsymbol{B}(\boldsymbol{x}_{s,u})\boldsymbol{u}(t) + \boldsymbol{g}(\boldsymbol{x}_{s,u}) - \bar{\dot{\boldsymbol{x}}}_u \tag{41}$$

where

$$\boldsymbol{A}(\boldsymbol{x}_{s,u}) = \left.\frac{\partial \boldsymbol{g}(\boldsymbol{x}_u)}{\partial \boldsymbol{x}_u}\right|_{\boldsymbol{x}_u = \boldsymbol{x}_{s,u}} = \begin{bmatrix} \boldsymbol{0}_{5\times1} & \boldsymbol{0}_{5\times5} \\ -\frac{3}{2}\sqrt{\frac{\mu}{a_{s,u}^5(t)}} & \boldsymbol{0}_{1\times5} \end{bmatrix} \tag{42}$$

Note that Eq. (41) is a linear time-varying system with respect to $\boldsymbol{x}_{p.u}$, and its solution is composed of two parts based on the linear system theory [29], i.e., the zero-input response and the zero-state response. For the zero-input response, it is obtained from the following differential equation [29],

$$\dot{\boldsymbol{x}}_{p,u}^{ZI}(t)=\boldsymbol{A}(\boldsymbol{x}_{s,u})\boldsymbol{x}_{p,u}^{ZI}(t) \tag{43}$$

i.e.,

$$\begin{cases}\dot{a}_{p,u}^{ZI}(t)=0;\\ \dot{e}_{p,u}^{ZI}(t)=0;\\ \dot{i}_{p,u}^{ZI}(t)=0;\\ \dot{\Omega}_{p,u}^{ZI}(t)=0;\\ \dot{\omega}_{p,u}^{ZI}(t)=0;\\ \dot{M}_{p,u}^{ZI}(t)=-\dfrac{3}{2}\sqrt{\dfrac{\mu}{a_{s,u}^{5}(t)}}a_{p,u}^{ZI}(t).\end{cases} \tag{44}$$

The solution to Eq. (44) is

$$\begin{cases}a_{p,u}^{ZI}(t)=a_{p,u}^{ZI}(t_0);\\ e_{p,u}^{ZI}(t)=e_{p,u}^{ZI}(t_0);\\ i_{p,u}^{ZI}(t)=i_{p,u}^{ZI}(t_0);\\ \Omega_{p,u}^{ZI}(t)=\Omega_{p,u}^{ZI}(t_0);\\ \omega_{p,u}^{ZI}(t)=\omega_{p,u}^{ZI}(t_0);\\ M_{p,u}^{ZI}(t)=M_{p,u}^{ZI}(t_0)+\dfrac{\sqrt{\mu}}{\bar{\dot{a}}_u}\left[a_{s,u}^{-3/2}(t)-a_{s,u}^{-3/2}(t_0)\right]a_{p,u}^{ZI}(t_0).\end{cases} \tag{45}$$

Thus, the zero-input response is obtained from Eq. (45) and written in the state-space form,

$$\boldsymbol{x}_{p,u}^{ZI}(t)=\boldsymbol{\Phi}(t,t_0)\boldsymbol{x}_{p,u}^{ZI}(t_0) \tag{46}$$

where the state transition matrix (STM) $\boldsymbol{\Phi}(t,t_0)$ is

$$\boldsymbol{\Phi}(t,t_0)=\begin{bmatrix}1 & 0 & 0 & 0 & 0 & 0\\ 0 & 1 & 0 & 0 & 0 & 0\\ 0 & 0 & 1 & 0 & 0 & 0\\ 0 & 0 & 0 & 1 & 0 & 0\\ 0 & 0 & 0 & 0 & 1 & 0\\ \dfrac{\sqrt{\mu}}{\bar{\dot{a}}_u}\left[a_{s,u}^{-3/2}(t)-a_{s,u}^{-3/2}(t_0)\right] & 0 & 0 & 0 & 0 & 1\end{bmatrix} \tag{47}$$

In addition, based on the linear system theory [29], the zero-state response is

$$\begin{aligned}\boldsymbol{x}_{p,u}^{ZS}(t) &= \int_{t_0}^{t} \boldsymbol{\Phi}(t,\tau)\left\{\boldsymbol{B}[\boldsymbol{x}_{s,u}(\tau)]\boldsymbol{u}(\tau)+\boldsymbol{g}[\boldsymbol{x}_{s,u}(\tau)]-\bar{\dot{\boldsymbol{x}}}_u\right\}\mathrm{d}\tau \\ &\triangleq \boldsymbol{D}_1(t,t_0)+\boldsymbol{D}_2(t,t_0)-\boldsymbol{D}_3(t,t_0)\end{aligned} \tag{48}$$

where

$$\begin{cases}\boldsymbol{D}_1(t,t_0)=\int_{t_0}^{t}\boldsymbol{\Phi}(t,\tau)\boldsymbol{B}[\boldsymbol{x}_{s,u}(\tau)]\boldsymbol{u}(\tau)\,\mathrm{d}\tau \\ \boldsymbol{D}_2(t,t_0)=\int_{t_0}^{t}\boldsymbol{\Phi}(t,\tau)\boldsymbol{g}[\boldsymbol{x}_{s,u}(\tau)]\,\mathrm{d}\tau \\ \boldsymbol{D}_3(t,t_0)=\int_{t_0}^{t}\boldsymbol{\Phi}(t,\tau)\bar{\dot{\boldsymbol{x}}}_u\,\mathrm{d}\tau\end{cases} \tag{49}$$

For $\boldsymbol{D}_2(t,t_0)$, substituting Eq. (47) and Eq. (39) into Eq. (49) yields

$$\boldsymbol{D}_2(t,t_0)=\int_{t_0}^{t}\boldsymbol{\Phi}(t,\tau)\boldsymbol{g}[\boldsymbol{x}_{s,u}(\tau)]\,\mathrm{d}\tau=\begin{bmatrix}\boldsymbol{0}_{5\times1}\\ \int_{t_0}^{t}\sqrt{\dfrac{\mu}{a_{s,u}^3(\tau)}}\,\mathrm{d}\tau\end{bmatrix} \tag{50}$$

The solution to Eq. (50) is

$$\boldsymbol{D}_2(t,t_0)=\begin{bmatrix}\boldsymbol{0}_{5\times1}\\ -\dfrac{2\sqrt{\mu}}{\bar{\dot{a}}_u}[a_{s,u}^{-1/2}(t)-a_{s,u}^{-1/2}(t_0)]\end{bmatrix} \tag{51}$$

For $\boldsymbol{D}_3(t,t_0)$, substituting Eq. (47) into Eq. (49) gives

$$\boldsymbol{D}_3(t,t_0)=\int_{t_0}^{t}\boldsymbol{\Phi}(t,\tau)\bar{\dot{\boldsymbol{x}}}_u\,\mathrm{d}\tau=\begin{bmatrix}\int_{t_0}^{t}\bar{\dot{a}}_u\,\mathrm{d}\tau\\ \int_{t_0}^{t}\bar{\dot{e}}_u\,\mathrm{d}\tau\\ \int_{t_0}^{t}\bar{\dot{i}}_u\,\mathrm{d}\tau\\ \int_{t_0}^{t}\bar{\dot{\Omega}}_u\,\mathrm{d}\tau\\ \int_{t_0}^{t}\bar{\dot{\omega}}_u\,\mathrm{d}\tau\\ \int_{t_0}^{t}\left\{\bar{\dot{M}}_u+\sqrt{\mu}\left[a_{s,u}^{-3/2}(t)-a_{s,u}^{-3/2}(\tau)\right]\right\}\mathrm{d}\tau\end{bmatrix} \tag{52}$$

The solution to Eq. (52) is

$$\boldsymbol{D}_3(t,t_0)=\begin{bmatrix} \dot{\bar{a}}_u(t-t_0) \\ \dot{\bar{e}}_u(t-t_0) \\ \dot{\bar{i}}_u(t-t_0) \\ \dot{\bar{\Omega}}_u(t-t_0) \\ \dot{\bar{\omega}}_u(t-t_0) \\ \left[\dot{\bar{M}}_u+\sqrt{\mu}a_{s,u}^{-3/2}(t)\right](t-t_0)+\dfrac{2\sqrt{\mu}}{\bar{a}_u}[a_{s,u}^{-1/2}(t)-a_{s,u}^{-1/2}(t_0)] \end{bmatrix} \tag{53}$$

For $\boldsymbol{D}_1(t,t_0)$, denote

$$\boldsymbol{D}_1(t,t_0)=\begin{bmatrix} D_{1,1}(t,t_0) \\ D_{1,2}(t,t_0) \\ D_{1,3}(t,t_0) \\ D_{1,4}(t,t_0) \\ D_{1,5}(t,t_0) \\ D_{1,6}(t,t_0) \end{bmatrix}=\begin{bmatrix} \int_{E_0}^{E} d_{1,1}(E,E_\tau)\,\mathrm{d}E_\tau \\ \int_{E_0}^{E} d_{1,2}(E,E_\tau)\,\mathrm{d}E_\tau \\ \int_{E_0}^{E} d_{1,3}(E,E_\tau)\,\mathrm{d}E_\tau \\ \int_{E_0}^{E} d_{1,4}(E,E_\tau)\,\mathrm{d}E_\tau \\ \int_{E_0}^{E} d_{1,5}(E,E_\tau)\,\mathrm{d}E_\tau \\ \int_{E_0}^{E} d_{1,6}(E,E_\tau)\,\mathrm{d}E_\tau \end{bmatrix} \tag{54}$$

Based on Eq. (47), Eq. (40), Eq. (49), and Eq. (8), the expressions of $\left\{d_{1,j}(E,E_\tau)\right\}\ (j=1,2,\ldots,6)$ are

$$\begin{cases} d_{1,1}(E_\tau)=\vartheta_1[\boldsymbol{x}_{s,u}(E_\tau)]u_r(E_\tau)+\vartheta_2[\boldsymbol{x}_{s,u}(E_\tau)]u_s(E_\tau) \\ d_{1,2}(E_\tau)=\vartheta_3[\boldsymbol{x}_{s,u}(E_\tau)]u_r(E_\tau)+\vartheta_4[\boldsymbol{x}_{s,u}(E_\tau)]u_s(E_\tau) \\ d_{1,3}(E_\tau)=\vartheta_5[\boldsymbol{x}_{s,u}(E_\tau)]u_w(E_\tau) \\ d_{1,4}(E_\tau)=\vartheta_6[\boldsymbol{x}_{s,u}(E_\tau)]u_w(E_\tau) \\ d_{1,5}(E_\tau)=\vartheta_7[\boldsymbol{x}_{s,u}(E_\tau)]u_r(E_\tau)+\vartheta_8[\boldsymbol{x}_{s,u}(E_\tau)]u_s(E_\tau)+\vartheta_9[\boldsymbol{x}_{s,u}(E_\tau)]u_w(E_\tau) \\ d_{1,6}(E,E_\tau)=a_{s,u}^{-3/2}(E)\vartheta_{10}[\boldsymbol{x}_{s,u}(E_\tau)]u_r(E_\tau)+\vartheta_{11}[\boldsymbol{x}_{s,u}(E_\tau)]u_r(E_\tau) \\ \qquad\qquad +a_{s,u}^{-3/2}(E)\vartheta_{12}[\boldsymbol{x}_{s,u}(E_\tau)]u_s(E_\tau)+\vartheta_{13}[\boldsymbol{x}_{s,u}(E_\tau)]u_s(E_\tau) \end{cases} \tag{55}$$

where

$$\begin{cases} \vartheta_1 = \dfrac{2\xi e\sqrt{a^3}}{\sqrt{\mu}\eta} s_\varphi,\ \vartheta_2 = \dfrac{2\xi\rho\sqrt{a^3}}{\sqrt{\mu}\eta},\ \vartheta_3 = \dfrac{\eta\xi\sqrt{a}}{\sqrt{\mu}} s_\varphi,\ \vartheta_4 = \dfrac{\xi\eta\sqrt{a}}{\sqrt{\mu}} \dfrac{e+(1+\rho)c_\varphi}{\rho} \\ \vartheta_5 = \dfrac{\xi\eta\sqrt{a}}{\sqrt{\mu}} \dfrac{c_{\varphi+\omega}}{\rho},\ \vartheta_6 = \dfrac{\xi\eta\sqrt{a}}{\sqrt{\mu}} \dfrac{s_{\varphi+\omega}}{\rho s_i},\ \vartheta_7 = -\dfrac{\xi\eta\sqrt{a}}{\sqrt{\mu}} \dfrac{c_\varphi}{e},\ \vartheta_8 = \dfrac{\xi\eta\sqrt{a}}{\sqrt{\mu}} \dfrac{1+\rho}{e\rho} s_\varphi \\ \vartheta_9 = -\dfrac{\xi\eta\sqrt{a}}{\sqrt{\mu}} \dfrac{c_i s_{\varphi+\omega}}{\rho s_i},\ \vartheta_{10} = \dfrac{2\xi e s_\varphi a^{3/2}}{\bar{\dot{a}}_u \eta},\ \vartheta_{11} = \dfrac{\xi\eta^2\sqrt{a}}{e\sqrt{\mu}} \dfrac{\rho c_\varphi - 2e}{\rho} - \dfrac{2\xi e s_\varphi}{\bar{\dot{a}}_u \eta}, \\ \vartheta_{12} = \dfrac{2\xi\rho a^{3/2}}{\bar{\dot{a}}_u \eta},\ \vartheta_{13} = -\dfrac{\xi\eta^2\sqrt{a}}{e\sqrt{\mu}} \dfrac{1+\rho}{\rho} s_\varphi - \dfrac{2\xi\rho}{\bar{\dot{a}}_u \eta} \end{cases} \tag{56}$$

where $\xi = [1 - e_0 \cos E(\tau)]/n_0$. In general, there is no closed-form solution to $\boldsymbol{D}_1(t, t_0)$, and the analytical approximate solution to $\boldsymbol{D}_1(t, t_0)$ is obtained in this section. For this purpose, $\left\{\vartheta_j[\boldsymbol{x}_{s,u}(E_\tau)]\right\}$ $(j = 1, 2, \ldots, 13)$ in Eq. (56) is approximated by using the truncated Fourier series in terms of eccentric anomaly,

$$\vartheta_j[\boldsymbol{x}_{s,u}(E_\tau)] = \sum_{k=0}^{N_{\vartheta,j}} q_{j,k} \cos(kLE_\tau) + \sum_{k=1}^{N_{\vartheta j}} q_{j,k+N_{\vartheta,j}} \sin(kLE) \tag{57}$$

where $N_{\vartheta,j}$ $(j = 1, 2, \ldots, 13)$ denotes the series truncation order, $q_{j,k}$ denotes the series expansion coefficient, which is also obtained from the discrete least-square approximation method [28]. Then, substituting Eq. (57) and the thrust series approximation Eq. (16) into Eq. (54) yields

$$\begin{cases} D_{1,1}(t,t_0) = \boldsymbol{q}_1^T \boldsymbol{G}(N_{\vartheta,1}, N_r)\boldsymbol{K}_r + \boldsymbol{q}_2^T \boldsymbol{G}(N_{\vartheta,2}, N_s)\boldsymbol{K}_s \\ D_{1,2}(t,t_0) = \boldsymbol{q}_3^T \boldsymbol{G}(N_{\vartheta,3}, N_r)\boldsymbol{K}_r + \boldsymbol{q}_4^T \boldsymbol{G}(N_{\vartheta,4}, N_s)\boldsymbol{K}_s \\ D_{1,3}(t,t_0) = \boldsymbol{q}_5^T \boldsymbol{G}(N_{\vartheta,5}, N_w)\boldsymbol{K}_w \\ D_{1,4}(t,t_0) = \boldsymbol{q}_6^T \boldsymbol{G}(N_{\vartheta,6}, N_w)\boldsymbol{K}_w \\ D_{1,5}(t,t_0) = \boldsymbol{q}_7^T \boldsymbol{G}(N_{\vartheta,7}, N_r)\boldsymbol{K}_r + \boldsymbol{q}_8^T \boldsymbol{G}(N_{\vartheta,8}, N_s)\boldsymbol{K}_s + \boldsymbol{q}_9^T \boldsymbol{G}(N_{\vartheta,9}, N_w)\boldsymbol{K}_w \\ D_{1,6}(t,t_0) = a_{s,u}^{-3/2}(t)\boldsymbol{q}_{10}^T \boldsymbol{G}(N_{\vartheta,10}, N_r)\boldsymbol{K}_r + \boldsymbol{q}_{11}^T \boldsymbol{G}(N_{\vartheta,11}, N_r)\boldsymbol{K}_r \\ \qquad\qquad + a_{s,u}^{-3/2}(t)\boldsymbol{q}_{12}^T \boldsymbol{G}(N_{\vartheta,12}, N_s)\boldsymbol{K}_s + \boldsymbol{q}_{13}^T \boldsymbol{G}(N_{\vartheta,13}, N_s)\boldsymbol{K}_s \end{cases} \tag{58}$$

where $\boldsymbol{q}_j = [q_{j,0}, \ldots, q_{j,2N_{\vartheta,j}}]^T$, $\boldsymbol{K}_\chi = [\kappa_{\chi,0}, \ldots, \kappa_{\chi,2N_\chi}]^T$ $(\chi = r, s, w)$, and

$$\boldsymbol{G}(N_1, N_2) = \int_{E_0}^{E} \boldsymbol{h}_{N_1}(E_\tau)\boldsymbol{h}_{N_2}^T(E_\tau)\,\mathrm{d}E_\tau \tag{59}$$

and where

$$\boldsymbol{h}_{N_k}(E_\tau) = \left[1, \cos(LE_\tau), \ldots, \cos(N_k LE_\tau), \sin(LE_\tau), \ldots, \sin(N_k LE_\tau)\right]^T \ (k = 1, 2) \tag{60}$$

The analytical expressions of $\boldsymbol{G}(N_1, N_2)$ can be obtained from Eq. (25)-Eq. (27). Thus, based on Eq. (58), Eq. (53), and Eq. (51), the zero-state response in Eq. (48) is obtained. Combined with the zero-input response in Eq. (46), the periodic term of orbital motion under thrust acceleration, $\boldsymbol{x}_{p.u}(t)$, in Eq. (41) is obtained. Furthermore, based on the periodic term of orbital motion under J_2 perturbation, $x_{p,J2}(t)$, in Eq. (30) -Eq. (35) and the secular orbital motion in Eq. (28), the continuous-thrust analytical state propagation under general thrust is obtained considering both the secular and periodic orbital motion.

5. Numerical examples

Suppose that the spacecraft is moving in an elliptical orbit, and the initial orbital elements are listed in Table 1. For simplicity, the series truncation orders in Eq. (16) and Eq. (57) are taken as the same values, respectively, i.e., $N_r = N_s = N_w = N_u$ and $N_{\vartheta,0} = N_{\vartheta,1} = \cdots = N_{\vartheta,13} = N_\vartheta$. In addition, for the numerical integration, the Runge-Kutta-Fehlberg (RKF78) is adopted, and the relative and the absolute error tolerances ("RelTol" and "AbsTol") are both set to be 10^{-12}.

Two simulation cases are considered to analyze the propagation accuracy of proposed methods: a) periodic thrust acceleration without including J_2 perturbation; b) non-periodic thrust acceleration including J_2 perturbation. For both cases, the fixed propagation time duration is taken as $5T_0$, where T_0 is the orbital period of the initial orbit. The series truncation orders in Eq. (16) and Eq. (57) are taken as $N_u = N_\vartheta = 16$, and the number of discrete points for the discrete least-square approximation is set to be 500 for computing the series expansion coefficients in Eq. (16) and Eq. (57).

Table 1 Initial orbital elements.

Orbital elements	Symbol	Spacecraft
Semi-major axis (km)	a	15000
Eccentricity	e	0.5
Inclination (deg)	i	30
Right ascension of ascending node (deg)	Ω	40
Argument of perigee (deg)	ω	50
True anomaly (deg)	φ	0

5.1. Case 1: periodic thrust acceleration without J_2 perturbation

The expression of the applied periodic thrust acceleration is (see Fig. 1)

$$\begin{cases} u_r(t) = 4e^{-3}\cos\left(\dfrac{\pi}{2}+\dfrac{2\pi}{T_0}t\right)(\text{m/s}) \\ u_s(t) = 3e^{-3}\sin\left(\dfrac{4\pi}{T_0}t\right)(\text{m/s}) \\ u_r(t) = 5e^{-3}\sin\left(\dfrac{2\pi}{T_0}t\right)\cos\left(\pi+\dfrac{2\pi}{T_0}t\right)(\text{m/s}) \end{cases} \tag{61}$$

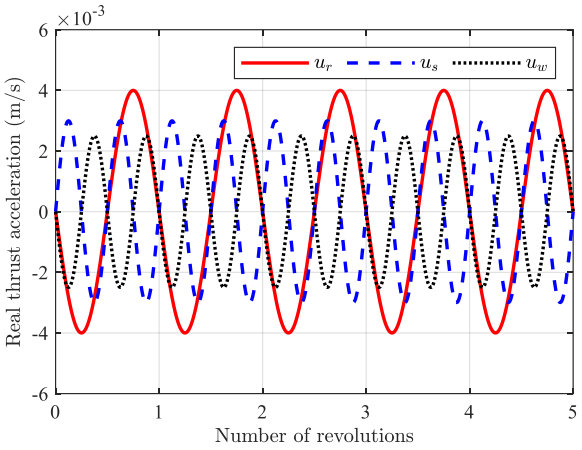

Fig. 1 Real thrust acceleration curves, case 1.

For the periodic thrust acceleration in Eq. (61) within each evolution, a truncated Fourier series approximation in terms of eccentric anomaly is obtained as Eq. (16) by using the discrete least-square approximation. The obtained thrust series approximation is also a periodic function within each revolution, thereby only 14 thrust coefficients are needed to analytically propagate the secular orbit motion based on the analysis in Ref. [24]. The analytical propagation of both the secular and periodic orbital motion is obtained based on the proposed method in Sec. 4, and the accurate orbital propagation is obtained by using the numerical integration method under the real thrust acceleration in Eq. (61). The results of orbital state propagation by the three methods are both plotted in Fig. 2, which clearly shows that considering both the secular and periodic orbital variations can be more effective in keeping up with the real orbital variation than considering only the secular orbital variation. In addition, the absolute errors of the results by the two analytical propagation methods compared with those by the numerical integration method are depicted in Fig. 3. The maximum absolute propagation errors of the two analytical propagation methods in the whole time period

are listed in Table 2, which shows the maximum propagation errors can be reduced by more than 80% by considering the periodic motion on the basis of the secular motion.

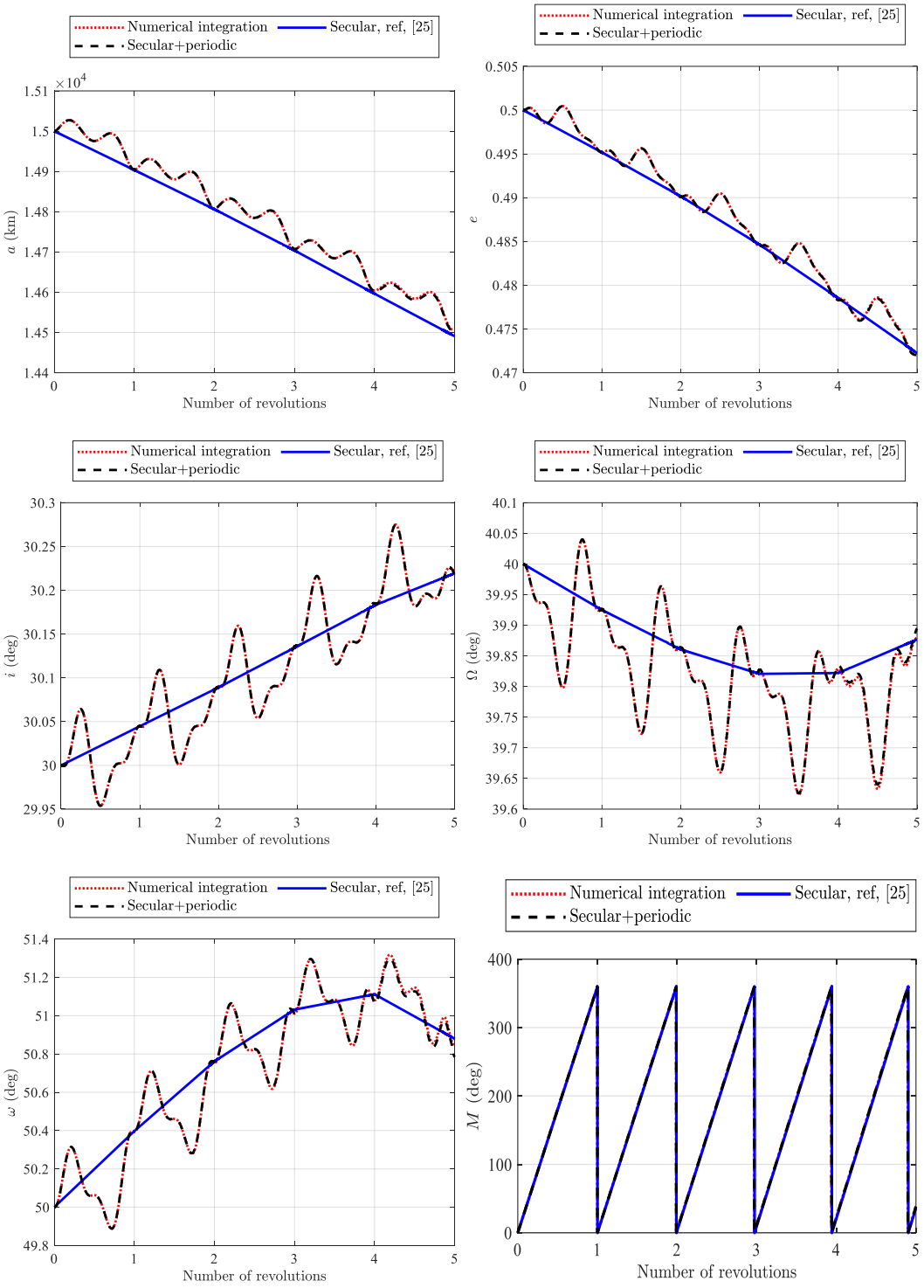

Fig. 2 Orbital state propagation by different methods, case 1.

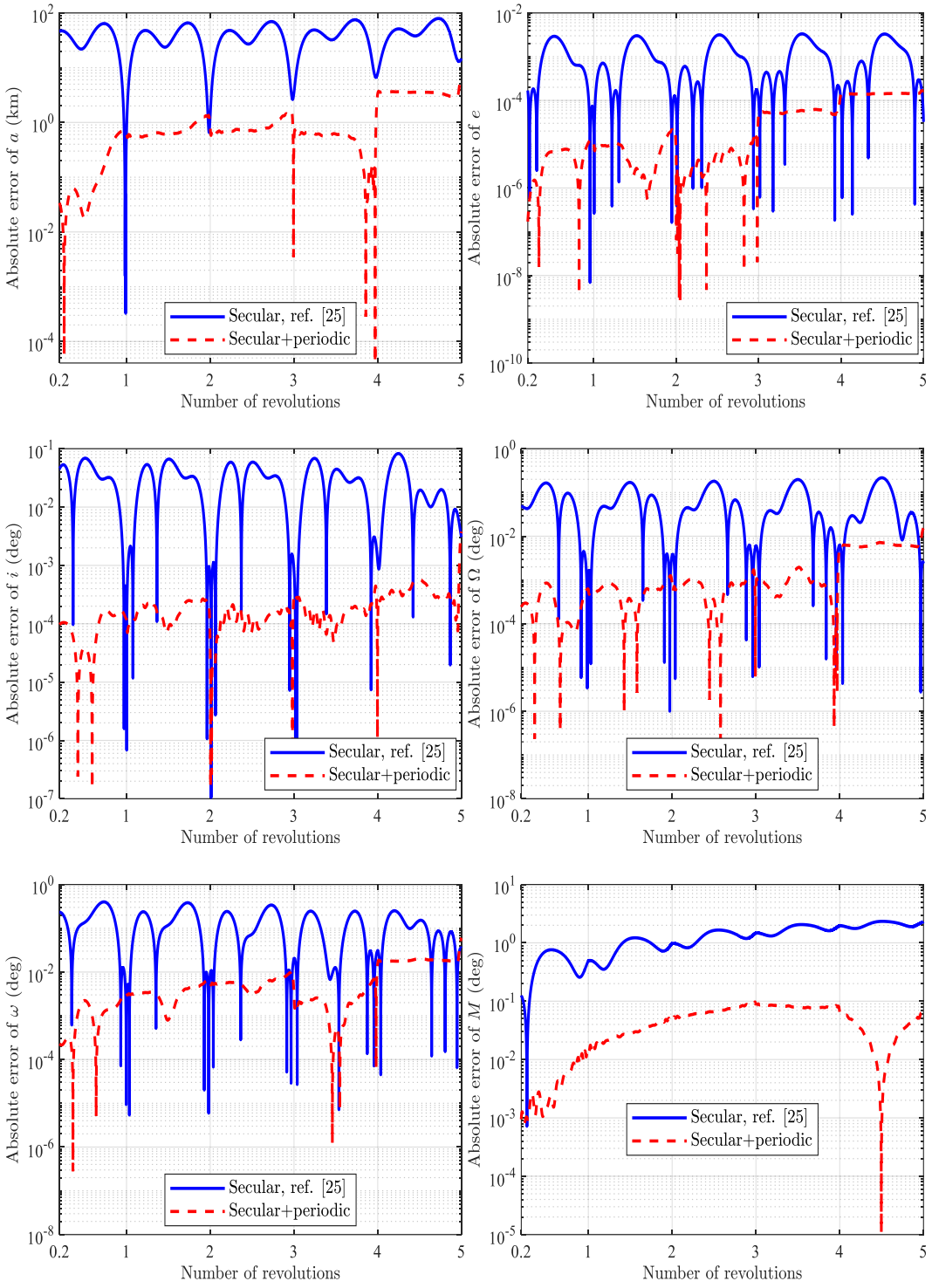

Fig. 3 Absolute propagation errors of different methods, case 1.

Table 2 Maximum absolute propagation errors od different methods, case 1.

Methods	Maximum absolute propagation errors					
	a (km)	e	i (deg)	Ω (deg)	ω (deg)	M (deg)
Secular, ref. [25]	79.1	3.32×10^{-3}	8.27×10^{-2}	2.17×10^{-1}	4.00×10^{-1}	2.34
Secular+periodic	7.22	1.71×10^{-4}	3.80×10^{-3}	1.55×10^{-2}	6.04×10^{-2}	9.68×10^{-2}
Reduced error (%)	90.9	94.9	95.4	92.8	84.9	95.9

5.2. Case 2: non-periodic thrust acceleration with J_2 perturbation

The expression of the applied non-periodic thrust acceleration is (see Fig. 4)

$$\begin{cases} u_r(t) = 5e^{-3}\left(1-\dfrac{t}{10T_0}\right)\cos\left(\dfrac{\pi}{2}+\dfrac{2\pi}{T_0}t\right)(\text{m/s}) \\ u_s(t) = 5e^{-3}\left(1-\dfrac{t}{10T_0}\right)\sin\left(\dfrac{4\pi}{T_0}t\right)(\text{m/s}) \\ u_r(t) = 5e^{-3}\left(1+\dfrac{t}{20T_0}\right)^2\sin\left(\dfrac{2\pi}{T_0}t\right)\cos\left(\pi+\dfrac{2\pi}{T_0}t\right)(\text{m/s}) \end{cases} \tag{62}$$

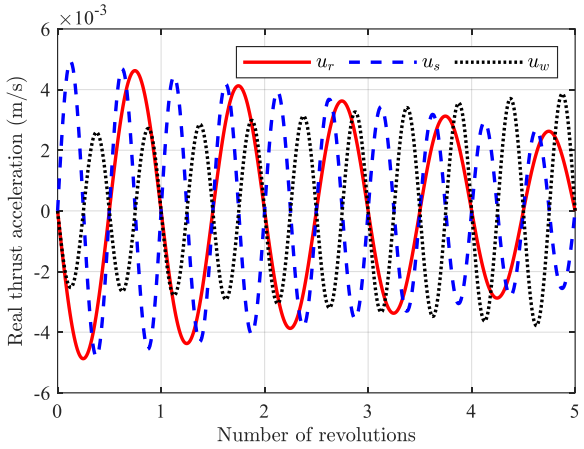

Fig. 4 Real thrust acceleration curves, case 2.

For the non-periodic thrust acceleration in Eq. (62) within each evolution, a truncated Fourier series approximation in terms of eccentric anomaly is also obtained as Eq. (16) by using the discrete least-square approximation. Since the obtained thrust series approximation is not a periodic function within each revolution, more than the 14 thrust coefficients in Ref. [24] are needed to analytically propagate the secular orbit motion based on the proposed method in Sec. 2. The analytical propagation of both the secular and periodic orbital motion is also obtained based on the proposed method in Sec. 4, and the accurate orbital propagation is obtained by using the numerical integration method under the real thrust acceleration in Eq. (61) and J_2 perturbation. The results of orbital state propagation by the three methods are both plotted in Fig. 5, which clearly shows that the real orbital variation under thrust acceleration and J_2 perturbation can be efficiently captured by the analytical propagation method considering both the secular and periodic orbital variations. In addition, the absolute

errors of propagation results by the two proposed analytical propagation methods compared with those by the numerical integration method are depicted in Fig. 6. The maximum absolute propagation errors of the two analytical propagation methods in the whole time period are listed in Table 3. The results of Table 3 show that by considering the periodic motion on the basis of the secular motion, the maximum propagation errors of the first five orbital elements and the mean anomaly can be reduced by more than 80% and 50%, respectively.

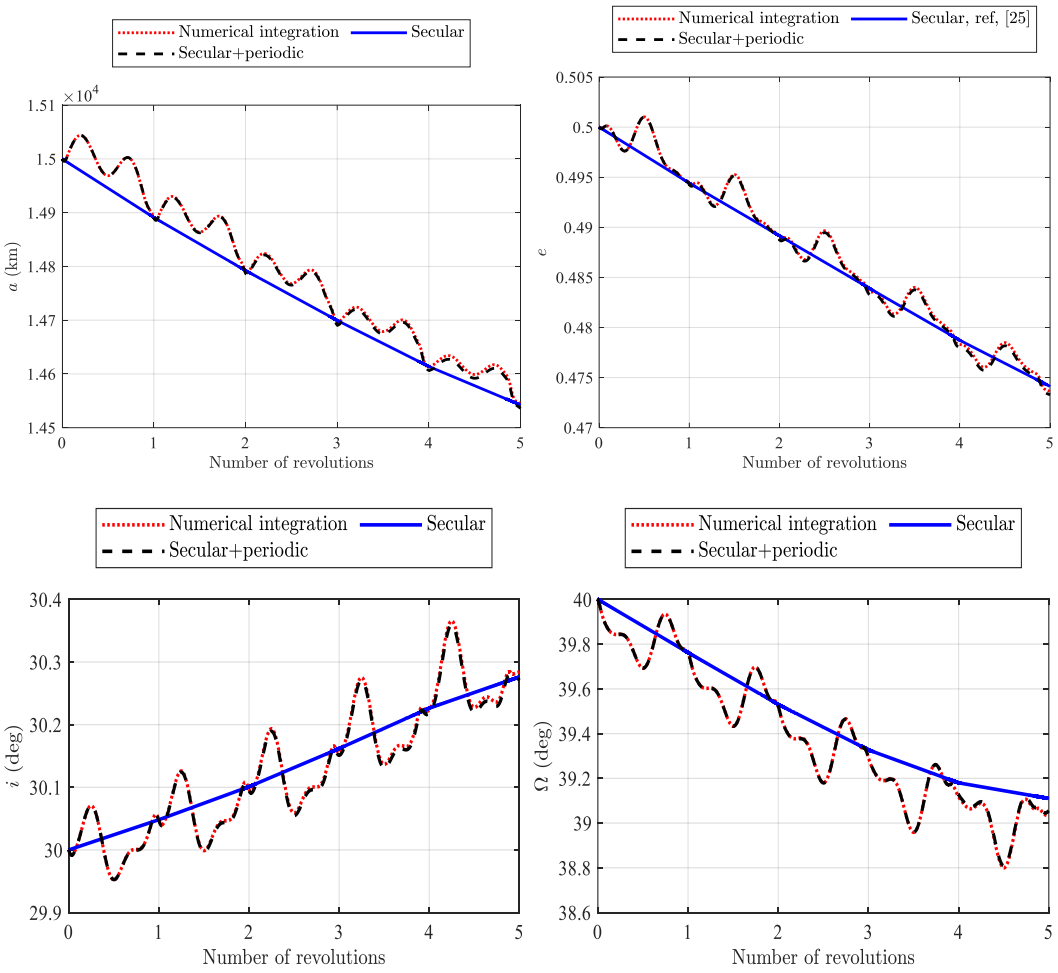

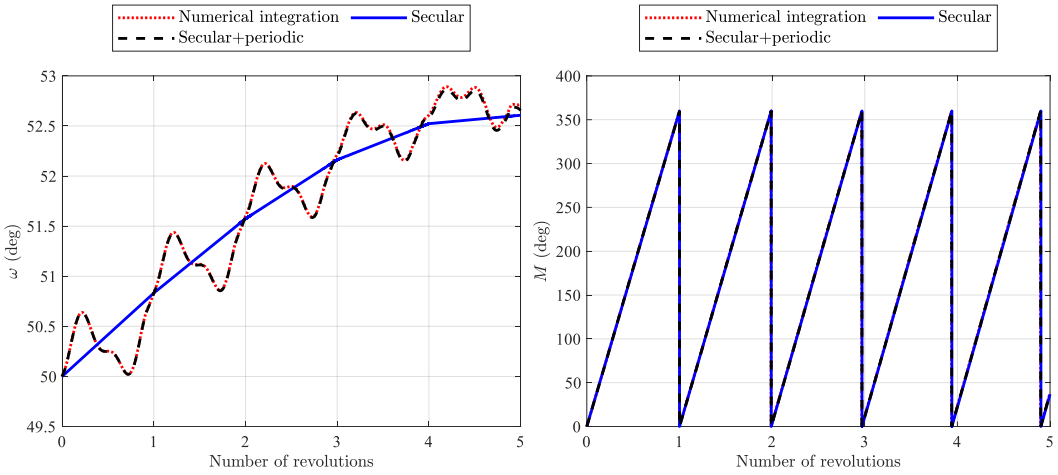

Fig. 5 Orbital state propagation by different methods, case 2.

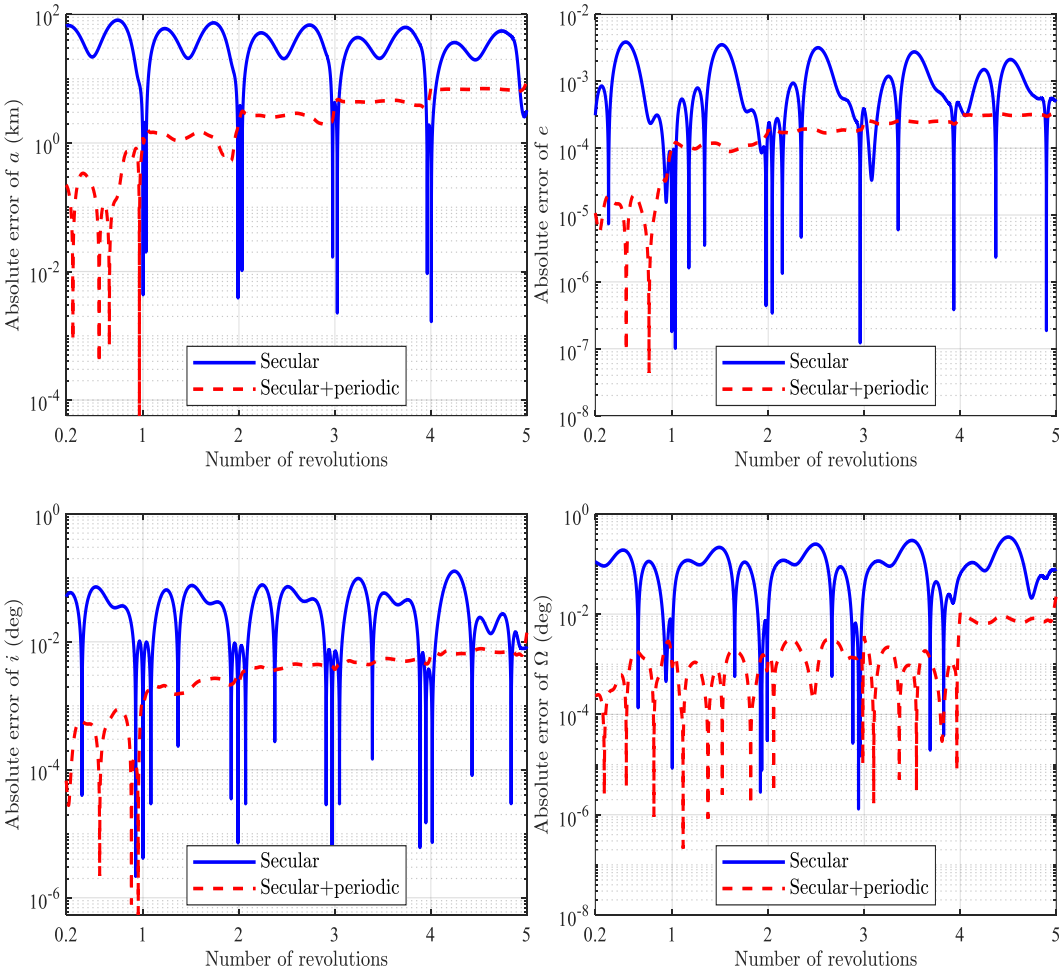

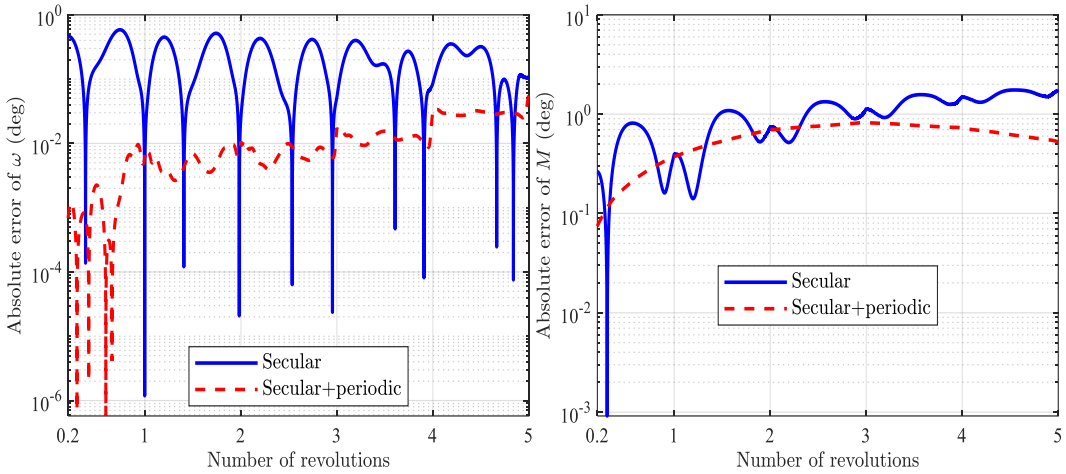

Fig. 6 Absolute propagation errors of different methods, case 2.

Table 3 Maximum absolute propagation errors od different methods, case 2.

Methods	Maximum absolute propagation errors					
	a (km)	e	i (deg)	Ω (deg)	ω (deg)	M (deg)
Secular	81.5	3.86×10^{-3}	1.27×10^{-1}	3.45×10^{-1}	5.86×10^{-1}	1.78
Secular+periodic	9.41	3.42×10^{-4}	1.39×10^{-2}	2.38×10^{-2}	6.10×10^{-2}	8.25×10^{-1}
Reduced error (%)	88.5	91.1	89.0	93.1	89.6	52.9

6. Conclusions

The continuous-thrust analytical state propagation for absolute orbital motion is proposed accounting for J_2 perturbation. The secular orbital motion and the periodic orbital motion are both considered. The proposed orbital propagation method is valid for both the periodic and non-periodic thrust acceleration. The real thrust acceleration is approximated by a truncated Fourier series in terms of eccentric anomaly. Two numerical cases are considered: periodic thrust without J_2 perturbation and non-periodic thrust with J_2 perturbation. The numerical results show that considering both the secular and periodic orbital variations can be more effective in keeping up with the real orbital variation than considering only the secular variation for the both cases. Compared with the secular orbital propagation, the maximum propagation errors relative to the numerical integration can be effectively reduced by additionally considering the periodic orbital variation.

References

[1] Bombardelli, Claudio, Giulio Baù, and Jesus Peláez. "Asymptotic solution for the two-body problem with constant tangential thrust acceleration." Celestial Mechanics and Dynamical Astronomy 110 (2011): 239-256.
[2] Zhang G, Ye D. Optimal short-range rendezvous using on–off constant thrust[J]. Aerospace Science and Technology, 2017, 69: 209-217.
[3] Tsien, H. S. "Take-off from satellite orbit." Journal of the American Rocket Society 23.4 (1953): 233-236.
[4] Battin, R. H., An Introduction to the Mathematics and Methods of Astrodynamics, rev. ed., AIAA Education Series, AIAA, Reston, VA, 1999, Chap. 8.
[5] Izzo, Dario, and Francesco Biscani. "Explicit solution to the constant radial acceleration problem." Journal of Guidance, Control, and Dynamics 38.4 (2015): 733-739.
[6] Kaki S, Akella M R. Spacecraft Rendezvous in Closed Keplerian Orbits Using Constant Radial Thrust Acceleration[J]. Journal of Guidance, Control, and Dynamics, 2023, 46(6): 1112-1125.
[7] Gonzalo J L, Bombardelli C. Multiple scales asymptotic solution for the constant radial thrust problem[J]. Celestial Mechanics and Dynamical Astronomy, 2019, 131(8): 37.
[8] Niccolai L, Quarta A A, Mengali G. Application of homotopy perturbation method to the radial thrust problem[J]. Astrodynamics, 2023, 7(2): 251-258.
[9] Benney, D., "Escape from a Circular Orbit Using Tangential Thrust," Journal of Jet Propulsion, Vol. 28, No. 3, 1958, pp. 167–169.
[10] Gao Y, Kluever C A. Analytic orbital averaging technique for computing tangential-thrust trajectories[J]. Journal of guidance, control, and dynamics, 2005, 28(6): 1320-1323.
[11] Perkins F M. Flight mechanics of low-thrust spacecraft[J]. Journal of the Aerospace Sciences, 1959, 26(5): 291-297.
[12] Niccolai L, Quarta A A, Mengali G. Orbital motion approximation with constant circumferential acceleration[J]. Journal of Guidance, Control, and Dynamics, 2018, 41(8): 1783-1789.
[13] Hernandez, S., and Akella, M. R., "Energy-Conserving Planar Spacecraft Motion with Constant-Thrust Acceleration," Journal of Guidance, Control, and Dynamics, Vol. 38, No. 12, 2015, pp. 2309–2323.
[14] Cao, J., Yuan, J. P., and Luo, J. J., "Orbital Motion Under Continuous Normal Thrust," Journal of Guidance, Control, and Dynamics, Vol. 37, No. 5, 2014, pp. 1691–1696.
[15] He, G., and Melton, R. G., "Analytic Approximation for Fixed-Angle Constant Thrust Trajectories via Linear Perturbation Theory," Journal of Guidance, Control, and Dynamics,Vol. 44, No. 1, 2021, pp. 163–171.
[16] Boltz F W. Orbital motion under continuous radial thrust[J]. Journal of Guidance, Control, and Dynamics, 1991, 14(3): 667-670.
[17] Boltz F W. Orbital motion under continuous tangential thrust[J]. Journal of Guidance, Control, and Dynamics, 1992, 15(6): 1503-1507.
[18] Roa J, Peláez J, Senent J. New analytic solution with continuous thrust: generalized logarithmic spirals[J]. Journal of Guidance, Control, and Dynamics, 2016, 39(10): 2336-2351.
[19] Di Mauro, G., Spiller, D., Carnà, S. F. R., and Bevilacqua, R., "Minimum-Fuel Control Strategy for Spacecraft Formation Reconfiguration via Finite-Time Maneuvers," Journal of Guidance, Control, and Dynamics, Vol. 42, No. 4, 2019, pp. 752–768.
[20] Zhou, D., and Zhang, G., "A Solution to Two-Point Boundary Value Problem for Power-Limited Rendezvous with Constant Thrust," Acta Astronautica, Vol. 69, Nos. 3–4, 2011, pp. 150–157.
[21] Gazzino C, Gurfil P. Optimization of satellite orbits with resonant cross-track control[J]. Journal of Guidance, Control, and Dynamics, 2019, 42(9): 1946-1961.
[22] Lin X, Zhang G. Analytical State Propagation for Continuous-Thrust Linear Relative Motion[J]. Journal of Guidance, Control, and Dynamics, 2022, 45(10): 1946-1957.
[23] Lin X, Zhang G. Second-Order State Propagation for Continuous-Thrust Relative Motion in J2-Perturbed Elliptic Orbits[J]. IEEE Transactions on Aerospace and Electronic Systems, 2022.
[24] Hudson, J. S., and Scheeres, D. J., "Reduction of Low-Thrust Continuous Controls for Trajectory Dynamics," Journal of Guidance, Control, and Dynamics, Vol. 32, No. 3, 2009, pp. 780–787.
[25] Ko, H. C., and Scheeres, D. J., "Essential Thrust-Fourier-Coefficient Set of Averaged Gauss

Equations for Orbital Mechanics," Journal of Guidance, Control, and Dynamics, Vol. 37, No. 4, 2014, pp. 1236–1249.
[26] Nie T, Gurfil P. Resonant Control of Satellite Orbits[J]. Journal of Guidance, Control, and Dynamics, 2021, 44(12): 2126-2142.
[27] Vallado D A. Fundamentals of astrodynamics and applications[M]. Springer Science & Business Media, 2001.
[28] Burden, R. L., Faires, J. D., and Burden, A. M., Numerical Analysis, 10th ed., Cengage Learning, Boston, 2015, Chap. 8.
[29] Chen, C. T., Linear System Theory and Design, Oxford Univ. Press, New York, 1999, Chap. 6.